

POTENTIAL THERMO-RESPONSIVE IONIC LIQUID AS DRAW SOLUTION IN FORWARD OSMOSIS APPLICATION

MOHD AMIRUL MUKMIN ABDULLAH*, MUHAMMAD SUHAIMI MAN,
PHANG SOOK NYAN, SYED M. SAUFI, SYAMSUL B. ABDULLAH

Faculty of Chemical and Natural Resources Engineering, Universiti Malaysia Pahang,
Gambang Campus, Lebuhraya Tun Razak, 26300,
Kuantan, Pahang Darul Makmur, Malaysia

*Corresponding Author: amirulmukmin731@gmail.com

Abstract

Desalination based on membrane technology is one of the approaches which has been extensively explored to tackle the challenge of increasing demand of clean water. Although reverse osmosis (RO) process has been applied for a long time, the promising forward osmosis (FO) membrane desalination is viewed as a potentially viable energy efficient performance technology. But, the main problem in FO process is the lack of suitable draw solutes that can be efficiently regenerated. A distinct advantage using thermo-responsive ionic liquids (ILs) is the efficient in regenerating the draw solute via thermally stimulation. These draw solutes achieved high water flux 1-butyl-3-methylimidazolium tetrafluoroborate ([Bmim][BF₄]) (0.71 LMH) and tetrabutylphosphonium trifluoroacetate ([P₄₄₄₄][CF₃COO]) (0.44 LMH) compared to NaCl (0.33 LMH). In this research, the phase separation via thermally stimulated liquid-liquid phase separation is achievable.

Keywords: Desalination, Draw solution, Forward Osmosis, Ionic liquid, Water flux.

1. Introduction

Rivers are the main source of water supply in Malaysia, contributing about 97% of total usage, with groundwater making up the balance. Together with an average annual rainfall of 3,000 mm, the country is rich in water resources and estimated of 566 billion m³ of water runs off into the river systems each year [1].

However, the demand for clean water is increasing rapidly due to the growth of population, expansion in urbanization, industrialization and agricultural irrigation. Lee et al. [1] reported that there are a few cities with high density of population such as Lembah Klang, Pulau Pinang and Johor Bahru, which required higher demands on water [1].

Besides that, the Malaysia's natural climate variability is heavily influenced by the Southeast Asia Maritime monsoon. During heavy rainy season, floods affect the lives of many people and cause great damage, destruction of property and water quality problems. Although many rivers are still in good condition, some are severely polluted by mud, sewage and solid waste [2]. Therefore, seawater desalination offers a reliable source of water supply that is not climate dependent [3, 4].

Based on studies by Greelee et al. [5], desalination processes fall into two main categories, thermal processes and membrane processes. The common processes for thermal process are Multi-Effect Distillation (MED) and Multi-Stage Flash (MSF). Many membrane-based modern technologies have been developed for seawater desalination and water reclamation. RO is a well-known process but is considerably expensive and not environmental friendly [6]. RO uses an average of prime electric energy 4 kW which shown in Table 1 below to produce one cubic meter of product water, whereby results in emission of 1.8 kg CO₂ per cubic meter of product water. In addition, fouling is inevitable in RO systems, thereby requiring the use of chemical cleaning agents and increasing the cost of water production by RO technology [7].

On the other hand, FO has been considered as an emerging membrane technology for water reuse and desalination of seawater. This spontaneous process demonstrates great potential to achieve energy efficient separations [10]. Furthermore, the major advantages of FO over RO are whether it operates at low or no hydraulic pressure at all, it can achieve high water recovery, and a lower tendency for membrane fouling. Generally, FO desalination processes involve two steps: osmotic dilution of the draw solution and fresh water generation from the diluted draw solution [11].

A careful analysis identified a low water flux, high reverse salt flux, and toxic by-products as the main drawbacks of using draw solutions. Therefore, a novel and appropriate draw solute that can overcome these limitations is essential. The ideal draw solutes for osmosis driven desalination that must have a high osmotic pressure in characteristics, zero toxicity, easy recovery and low cost. Many studies have been done to discover suitable draw solutes [12]. Akther et al. [13] explained that FO hybrid systems use thermos-responsive draw solutions, consume less total energy for desalting high-salinity waters and can be economically more feasible than other desalination technologies.

Many compounds have been proposed as thermally responsive draw solutes as listed in Table 2, including magnetic nanoparticles [14, 15], polymers [16], hydrogels [17], and ionic liquids [18, 19]. These draw solutes can be regenerated by various approaches, and they have certain advantages; however, they also involve significant drawbacks [20]. Therefore, there is a need to identify potential candidate of draw solution for FO system.

Ionic liquid (IL) are non-volatile, designable and a green solvent with wide liquid temperature range, excellent chemical and thermal stability [21-23]. All these unique characteristics are suitable for excellent draw solution. The comprehensive study in responsive IL as draw solutes focusing more on molecular structure design may attain better balance between hydrophilicity and hydrophobicity. There are two classification of thermo-responsive IL which are Upper Critical Solution Temperature (UCST) and Lower Critical Solution Temperature (LCST) behavior types [24].

The phase separations for UCST-type IL occur during cooling. Contrary to the UCST-type IL, the LCST-type IL phase separation occurs during heating. Interestingly, based on the mechanism of the LCST-type IL behaviour, more hydrophobic molecules facilitate easier regeneration and are perhaps more suitable for colder climate because both FO and regeneration are done at respective low temperatures. Otherwise, more hydrophilic (UCST-type IL) could be designed for use in the warmer climate [19].

Table 1. Comparison of estimated energy requirement for desalination technologies.

Desalination technique	Equivalent energy requirement (kWh/m ³)	Reference
FO	3-8	Moon and Lee [8]
RO	4-6	Moon and Lee [8]
MED	15-58	Semiat [9]
MSF	21-58	Semiat [9]

Table 2. Summary of several types of thermo-responsive draw solutes.

Types	Name	Findings	Reference
Magnetic nanoparticles	(PSSS-PNIPAM), (PNVCL), (POEGMA)	High water flux but poor regeneration and enhance membrane fouling.	Zhao et al. [14], Ling et al. [15] and Yildiz and Yildiz [25]
Polymer	(PPG), (PEI), OPT	Low osmotic pressure, low water flux and poor regeneration.	Kim et al. [16] and Chai and Hu [20]
Hydrogel	(PNIPAM) (PNIPAM-co-PSA)	Low water flux, and weak mechanical toughness.	Li et al. [17] Wei et al. [26] and Razmjou et al. [27]
Ionic liquids	(P ₄₄₄₄ DMBS), (P ₄₄₄₄ TMBS) (P ₄₄₄₈ Br), ([Hbet][NTf ₂])	High osmotic pressure and can be directly reused as draw solution without further treatment.	Cai et al. [18], Zhong et al. [19] and Cai and Hu [20], Hu et al. [28]

2. Methodology

2.1. Material

1-butyl-3-methylimidazolium tetrafluoroborate ([Bmim][BF₄]) (98%), tetrabutylphosphonium hydroxide (40 wt. %), trifluoroacetic acid for Synthesis and sodium chloride were purchased from Sigma Aldrich. The commercial FO

semipermeable membrane cellulose triacetate (CTA) flat sheet was purchased from Hydration Technologies Inc. (HTI, USA).

2.2. Ionic liquid synthesis

Tetrabutylphosphonium trifluoroacetate ($[P_{4444}][CF_3COO]$) was synthesized by neutralization process. Equal molar amount of tetrabutylphosphonium hydroxide and trifluoroacetic acid were added to a three-necked round bottom flask equipped with reflux condenser, a magnetic stirrer, and N_2 gas inlet and outlet. After 24 h of stirring, the solution was added to a dichloromethane (CH_2Cl_2)/water biphasic system in separatory funnel for extraction process as shown in Fig. 1. The dichloromethane layer was washed several times with distilled water. Then, the solution was evaporated using rotary evaporator as the dichloromethane layer was vaporised easily at its boiling point of $39.6\text{ }^\circ\text{C}$. After evaporation, the left solution is then dried in vacuum at $70\text{ }^\circ\text{C}$ for at least 24 hours before stored in centrifuge tube [29]. Lastly, ($[P_{4444}][CF_3COO]$) have been characterized using FTIR spectroscopic techniques to confirm the IL structure.

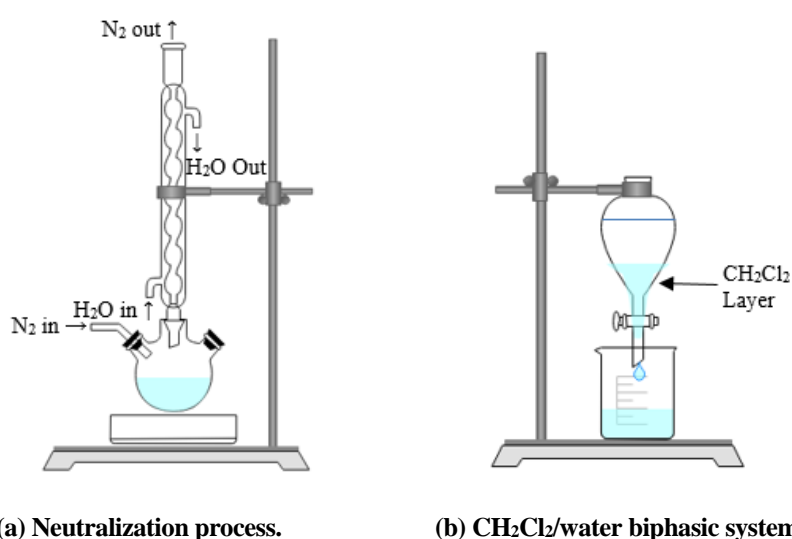


Fig. 1. Synthesis of ionic liquid experiment set up.

2.3. Determination of water flux

FO experiments were conducted through a lab-scale circulating set-up with the feed solution of 0.04 M NaCl and the draw solution of 0.087 M NaCl as a reference and is illustrated in Fig. 2. The same concentration of $0.087\text{ M (Bmim)}(BF_4)$ (UCST-type IL) and ($[P_{4444}][CF_3COO]$) (LCST-type IL) were prepared as draw solution. The amount of 300 mL feed solution and draw solution were used to carry out the FO process at room temperature. The peristaltic pump drive the draw and feed solutions to flow in a loop at each side of membrane cell with co-currently flow rate of 60.36 mL/min [30].

The water flux, J_w (LMH) in FO process was measured by the weight of feed solution monitored through balance that linked with a computer which able to

export the data automatically at a 5 minutes interval until the process accomplished, and calculated by Eq. (1) [31] where:

$$J_w = \frac{\Delta V}{A_m \cdot \Delta t} \quad (1)$$

The $\Delta V (L)$ is the volume change of the feed solution over a time $\Delta t (H)$ and $A_m (m^2)$ is the effective membrane surface area.

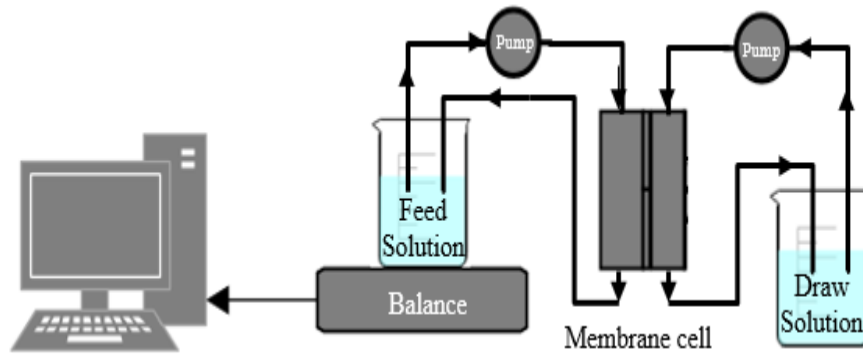


Fig. 2. Schematic diagram of FO setup.

2.4. Draw solution phase separation

Once FO process was completed, thermally stimulated phase separation was employed to separate water from the diluted IL draw solution. For UCST-type IL, the diluted draw solution was cooling down below the critical temperature to undergo liquid-liquid phase separation. Unlike UCST-type IL, the diluted LCST-type IL need to be heated up above the critical temperature to undergo liquid-liquid phase separation.

The diluted IL draw solution was poured into the rotary flask and evaporated using rotatory evaporator to reduce the amount of water present in the diluted IL draw solution. The remaining small amount of diluted IL draw solution was transferred into the specimen vial and placed in ice bath (UCST-type IL) or hot water bath (LCST-type IL).

2.5. Detecting IL traceable using UV-Vis spectroscopy

The traceable of both thermo-responsive IL draw solutions after phase separation was measured by using UV-Vis spectroscopy. The selection of this technique is because of the feature of ILs, visible and ultraviolet spectroscopy which is a good method in detecting the concentration of IL [32].

Sample solutions were prepared simply by taking the water phase of the draw solution. The optical transmittance spectra were measured using an UV-Vis-near infrared transmittance spectrometer at room temperature. The data of the water phase were collected at 190-400 nm. The light passed through the mixtures in a quartz cell with path length of 1 cm.

3. Results and Discussion

3.1. Infrared (IR) spectra of ([P4444][CF₃COO]) ionic liquid

Infrared (IR) spectrum obtained for ([P₄₄₄₄][CF₃COO]) is shown in Fig. 3. It was compared with the IR spectra of trifluoroacetic acid and tetrabutylphosphonium bromide as shown in Figs. A-1. and A-2 (*Appendix A*) to determine the present of functional groups.

In ([P₄₄₄₄][CF₃COO]), carboxyl group was presented by the peaks at the frequencies of 2959.27, 2932.68 and 2872.48 cm⁻¹, indicated the stretching of O-H. Another peak can be seen at the frequency of 1409.39 cm⁻¹. This band indicated the bending of O-H which also belonged to carboxyl group. There were peaks appeared between the frequencies of 1000-1400 cm⁻¹ and indicated the stretching of C-F.

Fluoro compound was presented and belonged to the halogen group. Besides that, the peaks appeared between the frequencies of 950-1250 cm⁻¹ shows that the bending of P-H and the phosphonium cation was presented. Therefore, based on the functional groups presented, it was confirmed that ([P₄₄₄₄][CF₃COO]) was successfully synthesised.

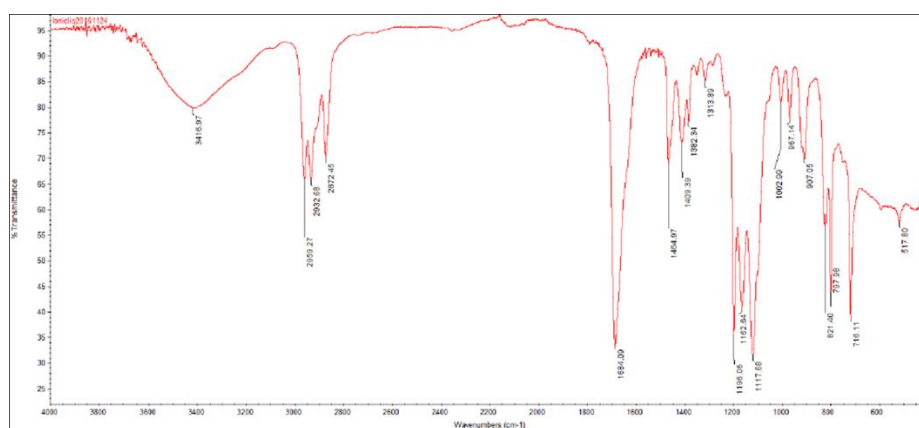


Fig. 3. Infrared spectrum of ([P₄₄₄₄][CF₃COO]).

3.2. Draw solution performance

The water flux was obtained with concentration of feed solution 0.040 M NaCl and 0.087 M of draw solution. NaCl draw solution was compared with two different types of thermo-responsive draw solution consist of LCST-type IL ([P₄₄₄₄][CF₃COO]) and UCST-type IL ([Bmim][BF₄]).

Figure 4 shows that 0.087 M ([Bmim][BF₄]) attained the highest water flux of 0.71 LMH compare to ([P₄₄₄₄][CF₃COO]) (0.44 LMH) and NaCl (0.33 LMH) with the same concentration of feed solution.

The water fluxes for the NaCl and ([P₄₄₄₄][CF₃COO]) draw solutes were relatively low compared to ([Bmim][BF₄]) because there were more water molecules drawn and diffused through the membrane by ([Bmim][BF₄]) draw solution side.

As studied for FO process, the difference in osmotic pressure across the membrane, the occurrence of extracranial or intracranial pressure, and the membrane performance will affect the water flux as well.

It was demonstrated that (Bmim)(BF₄) (UCST-type IL) have the highest draw ability as it is higher than ([P₄₄₄₄][CF₃COO]) (LCST-type IL) and NaCl solution.

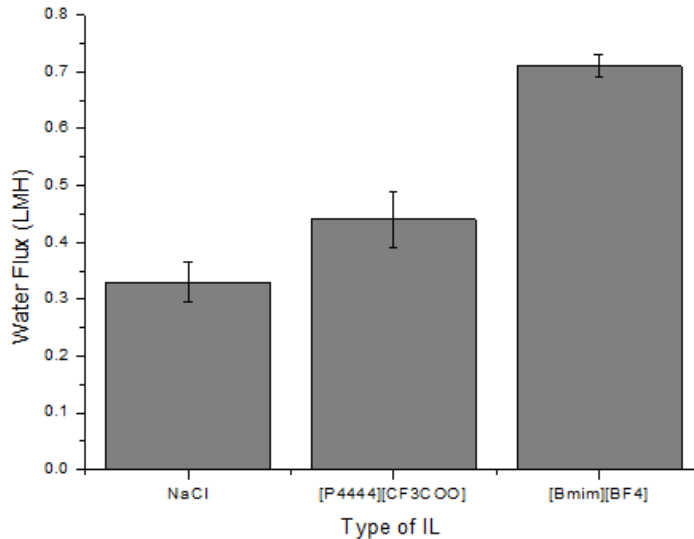


Fig. 4. Comparison of water flux at different draw solution.

3.3. Phase separation analysis

After conducting the FO process, the diluted IL draw solution underwent thermally stimulated phase separation experiment by heating above the critical temperature in water bath for LCST-type IL. The critical temperature of ([P₄₄₄₄][CF₃COO]) starting from 29 °C [24]. This temperature stimulated phase change behavior which is reversible and fast; by means ([P₄₄₄₄][CF₃COO]) formed homogenous mixtures with water at temperature below than 29 °C. Upon gentle heating, it was observed that the clear diluted IL draw solution turned to turbid and phase separation started. When the draw solution was heated above its critical temperature, a clear liquid-liquid phase separation appeared which formed an IL rich sediment phase and water rich supernatant phase as shown in Fig. 5.

Differing with LCST-type IL, ([Bmim][BF₄]) was cooling below the critical temperature about 6 °C in ice bath. The time taken for phase separation ([Bmim][BF₄]) as shown in Fig. 6 was about 20 minutes at temperature 3 °C compare to ([P₄₄₄₄][CF₃COO]) that take for an hour at temperature of 50 °C. However, when heating temperature increased, the time taken to complete phase separation decreased due to hydrogen bonding effect between LCST-type IL and water as shown in Fig. 7. This allowed the IL to be efficiently regenerated and reused. The phase separation temperature of the IL/water mixtures strongly depends on the hydrophobicity of the component ions as well as mixing ratio [29].

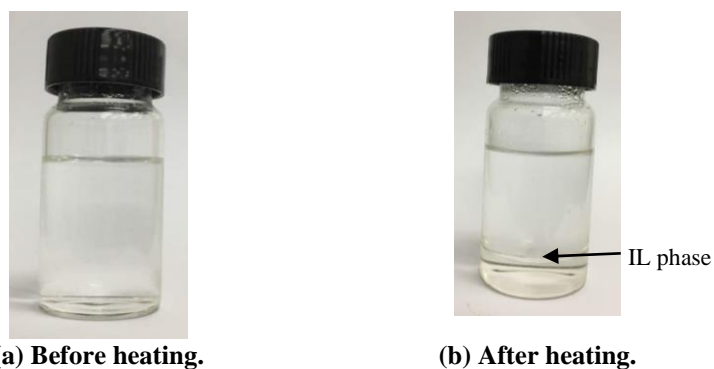


Fig. 5. Thermally stimulated phase separation process of LCST-type IL.

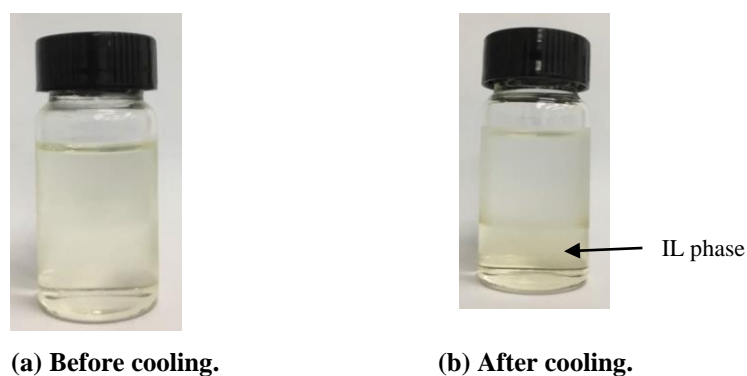


Fig. 6. Thermally stimulated phase separation process of UCST-type IL.

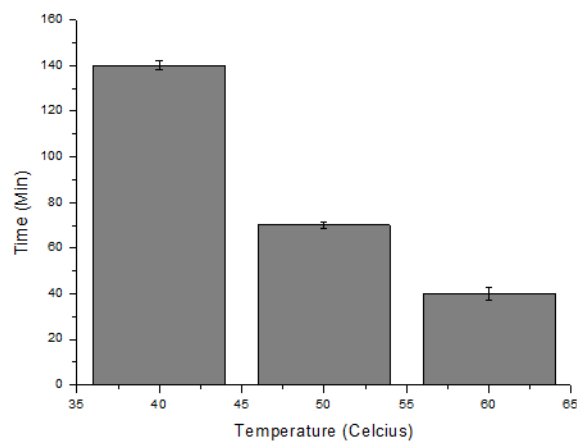


Fig. 7. Time for phase separation of ([P₄₄₄][CF₃COO]) -water mixture at different heating temperature.

3.4. Detecting of IL in water phase

By introducing the UV-Vis absorption spectra to detect traceable of IL in water phase, the result shown in Fig. 8 for thermo-responsive IL. The maximum

absorption wavelength (λ Max) were around 283 nm for ([Bmim][BF₄]) and 196 nm for ([P₄₄₄₄][CF₃COO]).

In short wavelength region as shown in Fig. 8, pure ([Bmim][BF₄]) and ([P₄₄₄₄][CF₃COO]) have typical absorption peaks at that point. Since pure H₂O has three typical weak peaks at 740, 765, 785 nm [33], the concentration of draw solution after phase separation can be detected quickly by a UV-Vis spectrometer.

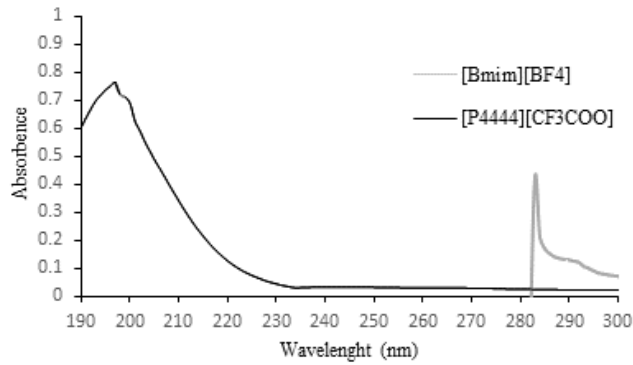


Fig. 8. UV-Vis absorption spectra.

4. Conclusions

Both LCST and UCST-type IL as draw solutions were successfully synthesized and performance evaluation was conducted in reflective water flux. ([Bmim][BF₄]) has high potential that can be use as draw solution due to high water flux 0.71 LMH compare to ([P₄₄₄₄][CF₃COO]) 0.44 LMH and both ILs achievable regeneration with thermally stimulate. Both IL traceable can be simply detected using UV-Vis spectrometer where λ Max was found around 283 nm for ([Bmim][BF₄]) and 196 nm for ([P₄₄₄₄][CF₃COO]).

Nomenclatures

A_m	Effective membrane surface area, m ²
J_w	Water flux, Lm ⁻² h ⁻¹
LMH	Water flux unit, Lm ⁻² h ⁻¹

Greek Symbols

Δt	Time change, h
ΔV	Volume change, L
λ	Wavelength, nm

Abbreviations

[Hbet][NTf ₂]	Betaine bis (trifluoromethyl sulfonyl) imide
OPT	Oligomeric poly (tetrabutylphosphonium styrene sulfonate)
P ₄₄₄₄ DMBS	Tetrabutylphosphonium 2,4- dimethylbenzene sulfonate
P ₄₄₄₄ TMBS	Tetrabutylphosphonium mesitylene sulfonate
P ₄₄₄₈ Br	Tributyloctyl-phosphonium bromide
PEI	N-acrylatepolyethylenimine
PNIPAM	Poly(N-isopropylacrylamide)

PNIPAM-co-PSA	Poly(N-isopropylacrylamide)-co-poly (sodium acrylate)
PNVCL	Poly (N-vinyl caprolactam)
POEGMA	Poly (oligo (ethylene glycol)-methacrylate)
PPG	Polypropylene glycol
PSSS-PNIPAM	Poly (sodium styrene-4-sulfonate)-co-poly(N-isopropylacrylamide)

References

1. Lee, K.E.; Mokhtar, M.; Hanafiah, M.M.; Halim, A.A.; and Badusah, J.J. (2016). Rainwater harvesting as an alternative water resource in Malaysia: potential, policies and development. *Journal of Cleaner Production*, 126, 218-222.
2. Abdullah, K. (2017). Integrated river basin management report. Integrated river basin management report. Retrieved April 20, 2017, from <https://www.water.gov.my/index.php/pages/view/708>.
3. Zhou, D.; Zhu, L.; Fu, Y.; Zhu, M.; and Xue, L. (2015). Development of lower cost seawater desalination processes using nanofiltration technologies-A review. *Desalination*, 376:109-116.
4. Jye, L.W. (2016). Seawater desalination is a viable option. Retrieved July 25, 2017, from <http://www.nst.com.my/news/2016/01/124850/seawater-desalination-viable-option>.
5. Greenlee, L.F., Lawler, D.F.; Freeman, B.D.; Marrot, B.; and Moulin, P. (2009). Reverse osmosis desalination : Water sources, technology , and today's challenges. *Water Research*, 43(9), 2317-2348.
6. Lee, S.; Boo, C.; Elimelech, M.; and Hong, S. (2010). Comparison of fouling behavior in forward osmosis (FO) and reverse osmosis (RO). *Journal of Membrane Science*, 365(1-2), 34-39.
7. Ray, S.S.; Chen, S.-S.; Nguyen, N.C.; Nguyen, H.T.; Li, C.-W.; Wang, J.; and Yan, B. (2016). Forward osmosis desalination by utilizing chlorhexidine gluconate based mouthwash as a reusable draw solute. *Chemical Engineering Journal*, 304, 962-969.
8. Moon, A.S.; and Lee, M. (2012). Energy consumption in forward osmosis desalination compared to other desalination techniques. *International Journal of Chemical and Molecular Engineering*, 6(5), 421-423.
9. Semiat, R. (2008). Energy issues in desalination processes. *Environmental Science and Technology*, 42(22), 8193-8201.
10. Law, J.Y.; and Mohammad, A.W. (2017). Employing forward osmosis technology through hybrid system configurations for the production of potable/pure water: A review. *Jurnal Teknologi*, 79(2), 125-135.
11. Zhao, S.; Zou, L.; Tang, C.Y.; and Mulcahy, D. (2012). Recent developments in forward osmosis: Opportunities and challenges. *Journal of Membrane Science*, 396, 1-21.
12. Ge, Q.; Ling, M.; Chung, T.-S. (2013). Draw solutions for forward osmosis processes: Developments, challenges, and prospects for the future. *Journal of Membrane Science*, 442, 225-237.

13. Akther, N.; Sodiq, A.; Giwa, A.; Daer, S.; Arafat, H.A.; and Hasan, S.W. (2015). Recent advancements in forward osmosis desalination: A review. *Chemical Engineering Journal*, 281, 502-522.
14. Zhao, Q.; Chen, N.; Zhao, D.; and Lu, X. (2013). Thermoresponsive magnetic nanoparticles for seawater desalination. *ACS Applied Materials and Interfaces*, 5(21), 11453-11461.
15. Ling, M.M.; Wang, K.Y.; and Chung, T.-S. (2010). Highly water-soluble magnetic nanoparticles as novel draw solutes in forward osmosis for water reuse. *Industrial and Engineering Chemistry Research*, 49(12), 5869-5876.
16. Kim, J.-j.; Kang, H.; Choi, Y.-S.; Yu, Y.A.; and Lee, J.-C. (2016). Thermo-responsive oligomeric poly(tetrabutylphosphonium styrenesulfonate)s as draw solutes for forward osmosis (FO) applications. *Desalination*, 381, 84-94.
17. Li, D.; Zhang, X.; Yao, J.; Simon, G.P.; and Wang, H. (2011). Stimuli-responsive polymer hydrogels as a new class of draw agent for forward osmosis desalination. *Chemical Communications*, 47(6), 1710-1712.
18. Cai, Y.; Shen, W.; Wei, J.; Chong, T.H.; Wang, R.; Krantz, W.B.; Fane, A.G.; and Hu, X. (2015). Energy-efficient desalination by forward osmosis using responsive ionic liquid draw solutes. *Environmental Science: Water Research and Technology*, 1(3), 341-347.
19. Zhong, Y.; Feng, X.; Chen, W.; Wang, X.; Huang, K.-W.; Gnanou, Y.; and Lai, Z. (2016). Using UCST ionic liquid as a draw solute in forward osmosis to treat high-salinity water. *Environmental Science and Technology*, 50(2), 1039-1045.
20. Cai, Y.; and Hu, X.M. (2016). A critical review on draw solutes development for forward osmosis. *Desalination*, 391, 16-29.
21. Ignat'ev N.V.; Finze, M.; Sprenger, J.A.P.; Kerpen, C.; Bernhardt, E.; and Willner, H. (2015). New hydrophobic ionic liquids with perfluoroalkyl phosphate and cyanofluoroborate anions. *Journal of Fluorine Chemistry*, 177, 46-54.
22. Pereira, A.B.; Araujo, J.M.M.; Oliveira, F.S.; Esperanca, J.M.S.S.; Lopes, J.N.C.; Marrucho, I.M.; Rebelo, L.P.N. (2012). Solubility of inorganic salts in pure ionic liquids. *The Journal of Chemical Thermodynamics*, 55, 29-36.
23. Vergara, M.A.V.; Lijanová, I.V.; Likhanova, I.V.; Xometl, O.O.; Viguera, D.J.; and Ramirez, A.J.M. (2015). Recycling and recovery of ammonium-based ionic liquids after extraction of metal cations from aqueous solutions. *Separation and Purification Technology*, 155, 110-117.
24. Kohno, Y.; and Ohno, H.; (2012). Temperature-responsive ionic liquid/water interfaces: Relation between hydrophilicity of ions and dynamic phase change. *Physical Chemistry Chemical Physics*, 14(15), 5063-5070.
25. Yildiz, I.; and Yildiz, B.S. (2015). Applications of thermoresponsive magnetic nanoparticles. *Journal of Nanomaterials*, Article ID 350596, 12 pages.
26. Wei, J.; Low, Z.-X.; Ou, R.; Simon, G.P.; and Wang, H. (2016). Hydrogel-polyurethane interpenetrating network material as an advanced draw agent for forward osmosis process. *Water Research*, 96, 292-298.
27. Razmjou, A.; Simon, G.P.; and Wang, H. (2013). Effect of particle size on the performance of forward osmosis desalination by stimuli-responsive polymer hydrogels as a draw agent. *Chemical Engineering Journal*, 215, 913-920.

28. Hu, X.; Cai, Y.; and Wang, R. (2015). A draw solute for forward osmosis. *European Patent EP2988853A1*. Nanyang Technological University.
29. Kohno, Y.; Arai, H.; Saita, S.; and Ohno, H. (2011). Material design of ionic liquids to show temperature-sensitive LCST-type phase transition after mixing with water. *Australian Journal of Chemistry*, 64(12), 1560-1567.
30. Long, Q.; Qi, G.; and Wang, Y. (2016). Evaluation of renewable gluconate salts as draw solutes in forward osmosis process. *ACS Sustainable Chemistry and Engineering*, 4(1), 85-93.
31. Achilli, A.; Cath, T.Y.; and Childress, A.E. (2010). Selection of inorganic-based draw solutions for forward osmosis applications. *Journal of Membrane Science*, 364(1-2), 233-241.
32. Torrecilla, J.S.; Rojo, E.; Oliet, M.; and Rodriguez, F. (2009). Determination of toluene, n-Heptane, [emim][ETSO4], and [bmim][MeSO4] ionic liquids concentrations in quaternary mixtures by uv-vis spectroscopy. *Industrial and Engineering Chemistry Research*, 48(10), 4998-5003.
33. Aono, M.; Imai, Y.; Abe, H.; Matsumoto, H.; and Yoshimura, Y. (2012). UV-Vis spectroscopic study of room temperature ionic liquid-water mixtures: N,N-diethyl-N-methyl-N-(2-methoxyethyl) ammonium tetrafluoroborate. *Thermochimica Acta*, 532, 179-182.
34. Linstrom, P.J.; and Mallard, W.G. (2017). *NIST chemistry webbook*. Washington, D.C.: National Institute of Standards and Technology (NIST).

Appendix A

Representation and Figures of Design Charts

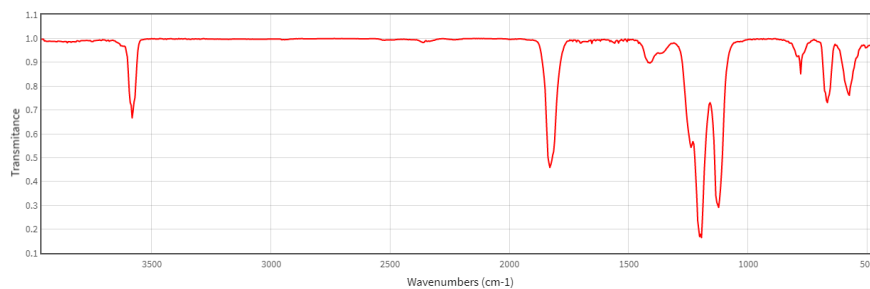


Fig. A-1. Infrared spectrum of trifluoroacetic acid [34].

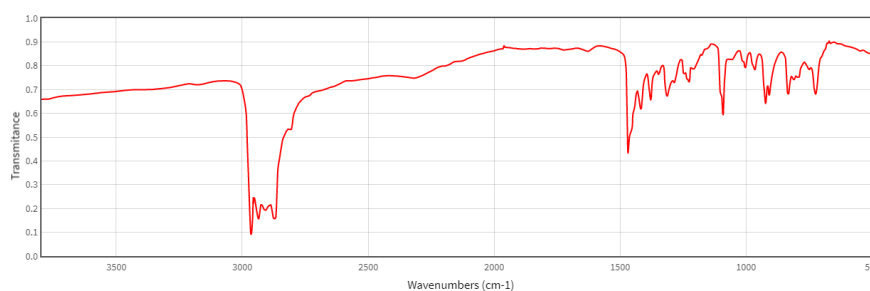


Fig. A-2. Infrared spectrum of tetrabutylphosphonium bromide [34].